Journal of Nuclear Materials 305 (2002) 97–105

journal of nuclear materials

www.elsevier.com/locate/jnucmat

A contribution to the Ru–Sn system

K. Ananthasivan [a], I. Kaliappan [a], P.R. Vasudeva Rao [a,*],
C. Sudha [b], A.L.E. Terrance [b]

[a] *Fuel Chemistry Division, Chemical Group, Indira Gandhi Centre for Atomic Research, Kalpakkam 603 102, India*
[b] *Physical Metallurgy Section, Metallurgy and Materials Group, Indira Gandhi Centre for Atomic Research, Kalpakkam 603 102, India*

Received 2 April 2002; accepted 3 August 2002

Abstract

The liquidus in the system Ru–Sn (35–90 at.% Sn) was experimentally determined by the spot technique in the temperature range 1173–1773 K. The liquidus in the tin rich region (90–100 at.% Sn) was determined by a new technique called the 'illuminated spot technique' in the temperature range 600–1823 K. The utility of this technique in the determination of steep liquidus boundaries was also demonstrated. The peritectic melting temperatures of the compounds Ru_3Sn_7 and Ru_2Sn_3 were also determined using the spot technique to be (1538 ± 4) and (1549 ± 10) K, respectively. A monotectic equilibrium was identified ((1570 ± 7) K, $\simeq$37 at.% Sn). The eutectic at (503 ± 1) K in the tin rich region (>98 at.% Sn) was measured using simultaneous differential thermal analysis. From the results obtained by high-temperature X-ray diffraction experiments, the compound $RuSn_2$ was found to decompose between 1348 and 1448 K.

1. Introduction

Experimental data on the solidus temperature of nuclear fuel materials (such as oxides, carbides and nitrides of U and Pu) are useful inputs for estimating the upper operational limit of the center line temperature of a reactor fuel element [1]. Data on the solidus and liquidus of alloys bearing actinide elements find application in the pyrochemical reprocessing of spent nuclear fuels. Information on the phase diagrams of the systems Sn–M (M = U, Pu, fission products) is useful for the liquid tin process [2]. Hence an experimental programme has been initiated in our Centre, in order to determine the solidus and liquidus temperatures in systems of relevance to fast reactor fuels. Since, the solidus and liquidus encountered in these systems occur in the temperature range 1000–2500 K, the 'spot technique' [3] – a method based on pyrometry – was chosen for these investigations. As part of these investigations, the solidus and liquidus boundaries in the system Ru–Sn were determined in this study.

Various authors investigated the Ru–Sn system [4–7]. The phase diagram proposed for the system Ru–Sn by Charles et al. [8] was based primarily on the work of Perring et al. [7]. Kawabata et al. [5] determined later the liquidus boundaries by thermal analysis, segregation method and solid state emf measurements (using calcia stabilized zirconia solid electrolyte). Susz [6] investigated the phase boundaries in this system by electron probe microanalysis (EPMA), differential thermal analysis (DTA) and X-ray diffraction (XRD). The phase diagram proposed by Susz [6], was revised later by Perring et al. [7]. The latter authors employed primarily DTA, EPMA and XRD in their investigations.

While Perring et al. [7] did not observe evidence in support of the peritectoid decomposition of Ru_2Sn_3, the phase diagram proposed by Susz [6] indicates the presence of the same. The liquidus temperatures measured by Perring et al. [7] are higher than those reported by Kawabata et al. [5]. The eutectic isotherms reported in Refs. [6,7] also differ. The results obtained by Perring et al. [7] showed that the intermetallic compounds viz.,

---

[*] Corresponding author. Tel.: +91-4114 40229/480098; fax: +91-4114 40365/480065.

E-mail address: vasu@igcar.ernet.in (P.R. Vasudeva Rao).

0022-3115/02/$ - see front matter © 2002 Elsevier Science B.V. All rights reserved.
PII: S0022-3115(02)01155-8

Ru_2Sn_3 and Ru_3Sn_7, are stable phases and $RuSn_2$ is probably metastable. The data on the liquidus temperatures in the composition range 90–100 at.% Sn are rather few, owing to the difficulties encountered in measuring this steep liquidus boundary, by using conventional methods.

In view of the above, phase boundaries of the system Ru–Sn in the temperature range 473–1823 K were determined in this study. In addition, experiments were also carried out in order to determine the temperature range over which $RuSn_2$ is stable.

2. Experimental

2.1. Starting materials

High purity ruthenium metal (99.99%) was procured in the form of fine powder (−325 mesh) from M/s. Leico Industries Inc., USA. Spectroscopic grade tin metal was supplied by M/s. BDH, Poole, UK, in the form of wire. Analar grade nitric acid was obtained from M/s. E. Merck (India) Ltd., Mumbai, India. Sodium peroxide was supplied by M/s. E. Merck, Germany. Sodium hydroxide was procured from M/s. E. Merck (India), Mumbai. Cupferron was procured from M/s. VEB Laborchemie Apolda, Germany.

2.2. Synthesis of alloys

Most of the alloy samples employed in this study were prepared by arc melting the elements in a triarc furnace supplied by M/s. Centorr Associates Inc., USA. Mixtures of Ru and Sn of desired stoichiometry were melted using a DC arc generated between a non-consumable, thoriated tungsten cathode and a water cooled, copper anode. The melting was done under argon containing about 4 ppm each of oxygen and moisture (IOLAR-2 grade argon gas, supplied by M/s. Indian Oxygen Ltd.) at a pressure of 1–10 Pa. To remove the residual oxygen in the arcing chamber, zirconium metal sponge was melted before melting the alloy components. The alloy button thus obtained was flipped and melted for about six times, in order to ensure homogenization. Some of these buttons were wrapped in a tantalum foil and encapsulated in quartz ampoules at a pressure of about 1×10^{-3} Pa. These samples were then annealed at 1073 K for 15 days. A custom made, nichrome wire wound resistance furnace was used for this purpose. The temperature of this furnace was controlled within ±1 K by using a proportional integral derivative temperature controller.

In some experiments the alloys were made in situ during the measurement. The details of the apparatus used in the present study for measuring the solidus and liquidus temperatures using the spot technique are given in Section 2.4.

2.3. Principle of the spot technique

The basic principle behind the spot technique is described in detail elsewhere [3]. Many binary phase diagrams involving refractory metals were determined using this technique [9–16]. A Knudsen cell containing the sample is heated by either radio frequency (RF) induction or electron bombardment [13]. Upon melting, reflectivity and emissivity [14] of the sample (solid alloy) change due to liquefaction. This liquid globule acts as a mirror and reflects the image of the orifice of the Knudsen cell as a black spot. When the temperature (and composition) of the alloy falls in a two-phase field, where solid and liquid coexist, several small black spots appear. These small spots coalesce to form a complete spot, once the sample is heated to the liquidus temperature.

The meniscus of the completely molten alloy can be convex, concave or planar depending on the wetting characteristics of the liquid alloy. The size and relative position at which the image is located along the optical axis of this liquid mirror depend on the shape of this liquid surface [13]. Garg [15] explained the mechanism of appearance of the spot as well as the dependence of the size of the spot on the geometry of the liquid surface, by assuming paraxial conditions. Awasti et al. [16] used the spot technique for measuring the wetting angle of liquid mercury on graphite.

Recent work carried out in our laboratory [17] showed that the spot technique can be extended to temperatures lower than 1073 K by using an external illumination procedure. This technique is essentially the same as the conventional spot technique but for the reversal in the direction of illumination. In this procedure, the contents inside the Knudsen cell are illuminated through the orifice by means of an external light source. When this technique is employed, a bright spot is observed instead of a black spot. Thus the illuminated spot technique does not require the internals of the Knudsen cell to be self-illuminating and it can be used for the investigation of solid–liquid equilibria at any temperature as long as the luminous intensity of the external light source is higher than that of the internals of the Knudsen cell.

2.4. Experimental assembly

A schematic diagram of the experimental assembly used in the present study is shown in Fig. 1. The details of construction of the Knudsen cell used in the present study are illustrated in Fig. 2. The apparatus essentially comprised a vacuum chamber and a sample support assembly. This chamber was evacuated by a diffusion

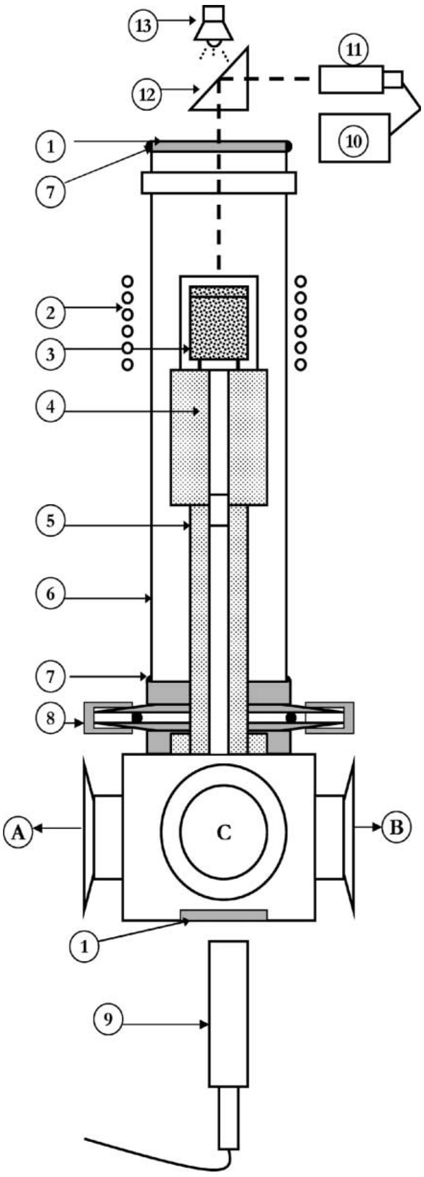

Fig. 1. A schematic diagram showing the experimental system used for the measurement of solidus and liquidus temperatures by the spot technique: (1) quartz window, (2) RF coil, (3) Knudsen cell, (4) graphite support tube, (5) stainless steel support tube, (6) quartz tube, (7) torr seal, (8) NW 40 coupling, (9) pyrometer lens assembly, (10) video monitor, (11) long distance microscope, (12) right angled prism, (13) light source, (A) port for penning gauge, (B) port for evacuation and (C) port for thermocouple.

pumping system (M/s. Balzers GmbH, Switzerland). A RF generator (11 kW, 400 kHz, M/s. Electronics Devices, Mumbai, India) was used to heat the Knudsen cell. Temperatures above 1173 K were measured using a pyrometer (M78, M/s. Micron, USA). An image capture system comprising a long distance microscope (QM1, M/s. Questar, Inc., USA), a charge coupled device camera (WAT 207 A, M/s. Watec Co. Ltd., Japan) and a video monitor were used to view and record the appearance of the 'spot'.

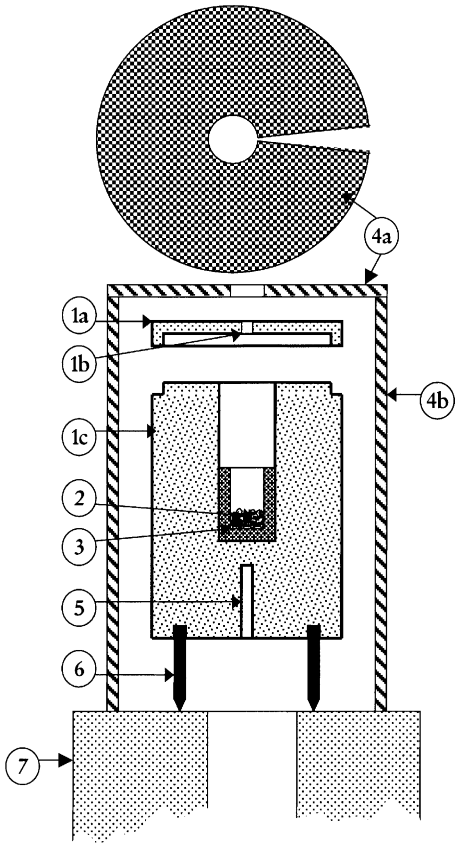

Fig. 2. Details of the Knudsen cell employed in high temperature spot experiments: (1a) Knudsen cell lid, (1b) Knudsen cell orifice, (1c) Knudsen cell (2) sample, (3) ceramic cup, (4a) top radiation shield, (4b) concentric radiation shield, (5) black body hole, (6) tungsten legs and (7) graphite support tube.

A conventional Knudsen cell was used for measurements above 1173 K. Temperatures in the range 473–1173 K were measured using a 'K-type' thermocouple which was inserted into the graphite Knudsen cell through its bottom.

2.5. Experimental procedure

In a typical 'high-temperature experiment' about 200–500 mg of the sample were taken in a cup made out of thoria. These cups were made 'in-house' from a sinteractive thoria powder [18]. The sample was heated at a rate of 10 K min^{-1} by RF induction. A pressure of 1×10^{-3} Pa was maintained during the experiment. A heating rate of 10 K min^{-1} was employed to reach a temperature, which was about 100 K less than the solidus temperature. Subsequently the sample was heated at a rate of

1 K min^{-1} up to its liquidus temperature. The temperature corresponding to the appearance of the broken spot (peritectic/eutectic/monotectic) as well as the complete spot (liquidus) were recorded. These measurements were made during the heating as well as the cooling cycle.

A procedure similar to that described above was used in the illuminated spot experiment. However, in these trials the source of light (a fluorescent lamp) above the Knudsen cell orifice was turned on and the temperature corresponding to the appearance of the 'bright spot' was measured by using a K-type thermocouple.

The simultaneous differential thermal analysis (SDTA) of the alloys with 90–98 at.% Sn was determined by a thermal analyzer TGA/SDTA851^{e}, supplied by M/s. Mettler Toledo, Switzerland. The sample was held in an alumina cup in a stream of high purity argon gas (less than 4 ppm each of moisture and oxygen). The temperature corresponding to the eutectic transformation was determined by employing three different heating rates viz., 2, 5 and 10 K min^{-1}. The onset temperature was then determined by extrapolating the above data to a heating rate of 0 K min^{-1}. The apparatus used in the illuminated spot experiments as well as the thermal analyzer were calibrated by measuring the melting points of pure In, Sn, Pb, Bi and Au.

2.6. Chemical assay of the alloys used in the present investigation

In order to determine the concentration of tin in the Ru–Sn alloys, a wet chemical procedure was employed. The alloy sample was solubilised by fusing it with sodium hydroxide and sodium peroxide taken in a nickel crucible at about 1073 K. The details of the fusion procedure are described elsewhere [20]. Subsequently the fused mass was quantitatively dissolved in 8 N HCl. The tin present in this solution was estimated gravimetrically as SnO_2 by incinerating the precipitate obtained by treating it with an excess of cupferron [19] at 1073 K for 1 h.

Various intermetallic phases present in the Ru–Sn alloys were analysed by XRD. The high-temperature phase transition in some alloy samples was investigated by using an X-ray diffractometer (XPERT MPD system) with a high-temperature attachment, supplied by M/s. Philips, Netherlands. This instrument was calibrated using a standard silicon sample. The microstructure of some of the alloys studied in the present investigation was obtained by scanning electron microscopy (XL 30 ESEM, TMP, Netherlands). Energy dispersive analysis of the characteristic X-rays (EDAX) was used to determine the composition of the different phases present in these samples.

3. Results

3.1. Validation of the high-temperature experiments

The pyrometer was calibrated against a standard black body source (M/s. Mikron Inc., USA, Model No. M 390). In order to ascertain the accuracy of the

Table 1
Solidus and liquidus temperatures in the system Ru–Sn

at.% Sn	T (K)	Liquidus (K)	at.% Sn	T (K)	Liquidus (K)	at.% Sn	T (K)	Liquidus (K)
18.09	1565^{M}	>1845	57.69	1540^{P1}	1617	77.22	–	1535
27.65	–	>1845	64.66	1569^{M}	–	74.44	–	1519
28.07	1550^{M}	>1845	64.66	1567^{M}	–	74.44	–	1524
32.34	1568^{M}	>1845	66.44		1602	77.32	–	1478
32.37	1555^{M}	>1845	66.44	1533^{P2}	–	80.28	–	1424
35.92	1585^{M}	1656	65.97	1535^{P2}	–	88.14	–	1339
44.82	1564^{M}	–	65.97	1534^{P2}	–	88.17	–	1363
44.86	1535^{P1}	–	66.93	1535^{P2}	1556	88.80	(501) 508^{*E}	
44.86	1528^{P1}	1595	68.10	1535^{P2}	1550	89.37	–	1343
44.86	1545^{P1}	–	68.10	1540^{P2}	–	89.37	–	1333
45.16	1548^{P1}	1591	68.12	1535^{P2}	1545	89.37	–	1349
48.46	1545^{P1}	–	69.50	1539^{P2}	1542	89.82	–	1228*
50.61	1541^{P1}	1555	69.50	1540^{P2}	–	89.82	508^{*E}	1209*
54.19	1553^{P1}	–	69.72	–	–	90.16	(504) 508^{*E}	
54.19	1539^{P1}	1557	70.33	–	1559	92.59	(503) 505^{*E}	1130*
56.69	1547^{P1}	–	70.61	–	1545	94.06	$(502)^{E}$	1100*
56.69	1536^{P1}	1557	70.76	–	1550	95.10	–	669*
						97.43	(501) 508^{*E}	640*
Au	$1335 \pm 2^{\$}$	Cu	$1357 \pm 2^{\$}$	Ni	$1727 \pm 2^{\$}$			

Temperature corresponds to: M – monotectic; P1 – peritectic (Ru_2Sn_3); P2 – peritectic (Ru_3Sn_7) and E – eutectic equilibria. * Data obtained by the illuminated spot technique; data in parenthesis refer to the values obtained by SDTA; $ – Melting point of pure elements.

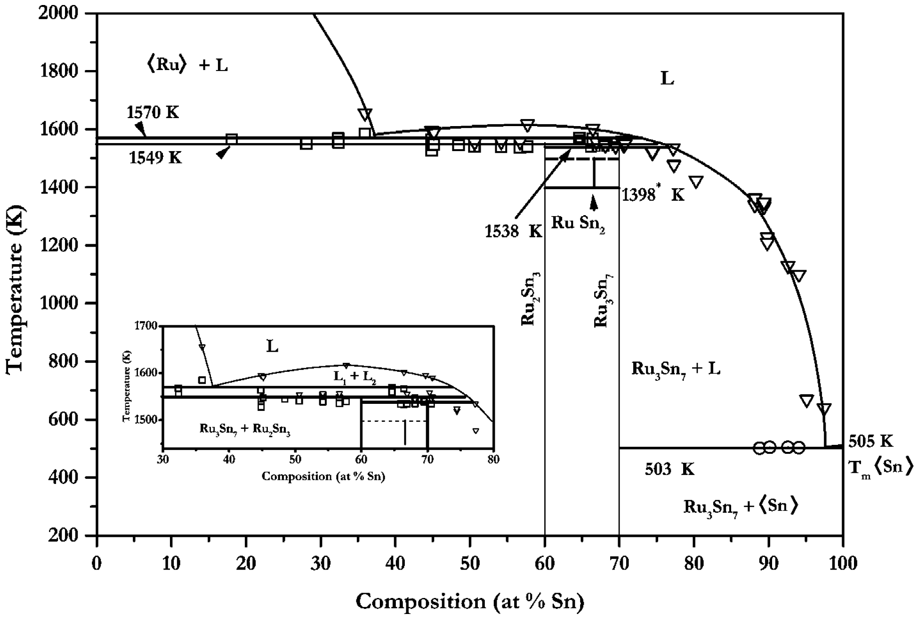

Fig. 3. Phase diagram of the Ru–Sn system. * $RuSn_2$ decomposes eutectoidally between 1348 and 1448 K.

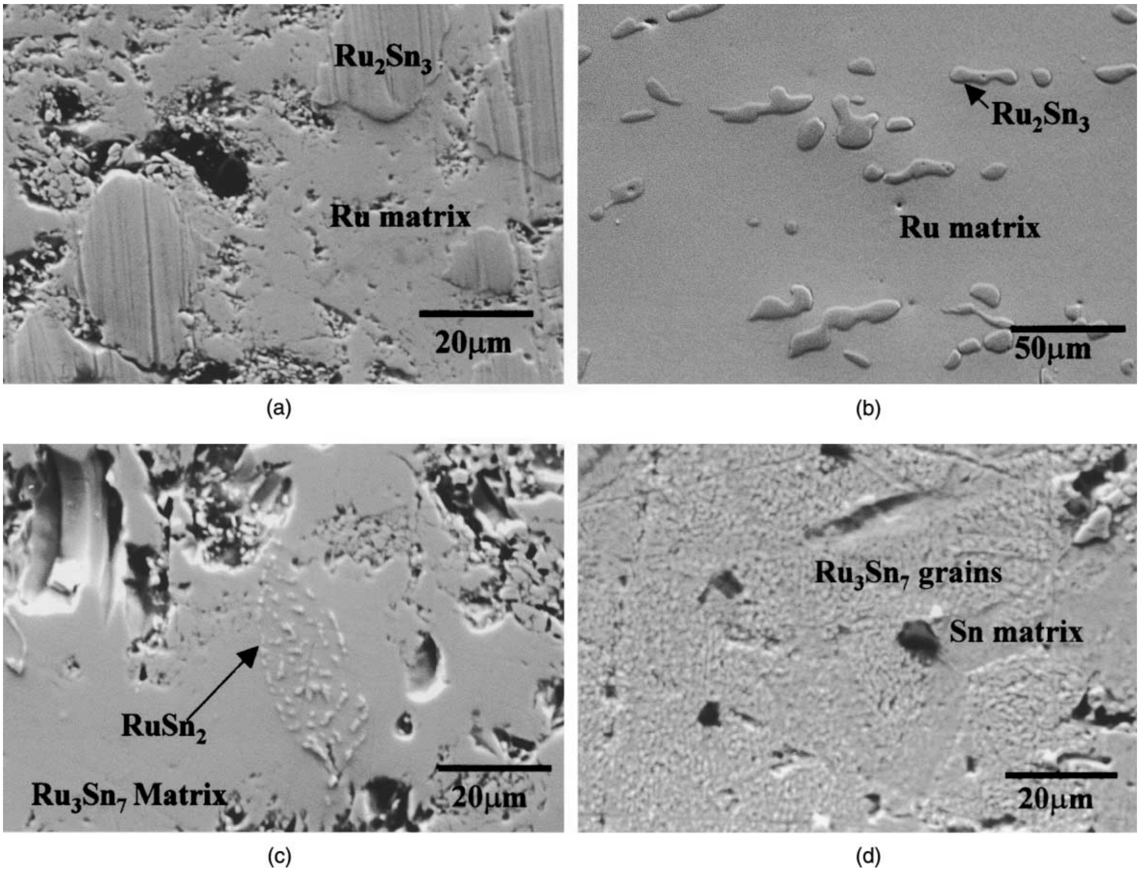

Fig. 4. SEM micrographs of Ru–Sn alloys: (a) $Ru_{0.69}Sn_{0.31}$, (b) $Ru_{0.51}Sn_{0.49}$, (c) $Ru_{0.31}Sn_{0.69}$ and (d) $Ru_{0.10}Sn_{0.90}$.

temperature measurement, the melting points of the pure metals, Au, Cu and Ni were determined. The mean of the values obtained in three measurements for each of these metals is indicated in Table 1. These values reveal that the melting temperatures could be determined within an uncertainty of 2 K, using the present experimental technique and apparatus in the temperature range 1350–1730 K. Results obtained in another study [21] indicated that the solidus and liquidus temperatures in binary alloys could be determined within an uncertainty of 3 K using the experimental apparatus employed in this study.

3.2. Chemical assay of the Ru–Sn alloys

Most of the Ru–Sn alloy samples employed in the present investigation showed loss of weight when the temperature of investigation exceeded 1573 K. It was surmised that this could be due to the preferential loss of tin under the experimental conditions. The low pressures employed during the experiments (1×10^{-3} Pa) probably caused the loss of tin (or its oxides) whose vapour pressure was higher than that of ruthenium [22] at temperatures above 1573 K. In order to confirm the above premise, some alloys were chemically assayed after the completion of the experiment. Earlier investigations carried out in our laboratory [20], revealed that it is possible to determine the tin content in Ru–Sn alloys within ±0.5 at.% by using a wet chemical method. The change in the composition of the alloys estimated from the weight loss (assuming only tin was lost due to vapourisation), agreed well with the experimentally determined composition of the alloys, within the limits of experimental error. Hence, it was concluded that the weight loss was only due to the vapourisation of tin (or one of the oxides of tin). The mean of the values of the composition at the beginning as well as end of the experiments is reported here. However, data pertaining to those samples in which more than 1 at.% loss was observed were rejected.

3.3. Peritectic, eutectic, monotectic and liquidus temperatures in the system Ru–Sn

The peritectic, eutectic, monotectic and liquidus temperatures obtained in the present investigation for the alloys in the Ru–Sn system are given in Table 1 as well as in Fig. 3. These data suggest that the following invariant equilibria exist in the system Ru–Sn:

(i) a monotectic equilibrium at (1570 ± 7) K (composition $\simeq$37 at.% Sn)

$$\text{Liquid 1} \xrightarrow{\text{Cooling}} \langle \text{Ru} \rangle + \text{Liquid 2}. \qquad (1)$$

(ii) peritectic decomposition of Ru_2Sn_3 at (1549 ± 10) K

$$\text{Liquid} + \langle \text{Ru} \rangle \xrightarrow{\text{Cooling}} \text{Ru}_2\text{Sn}_3. \qquad (2)$$

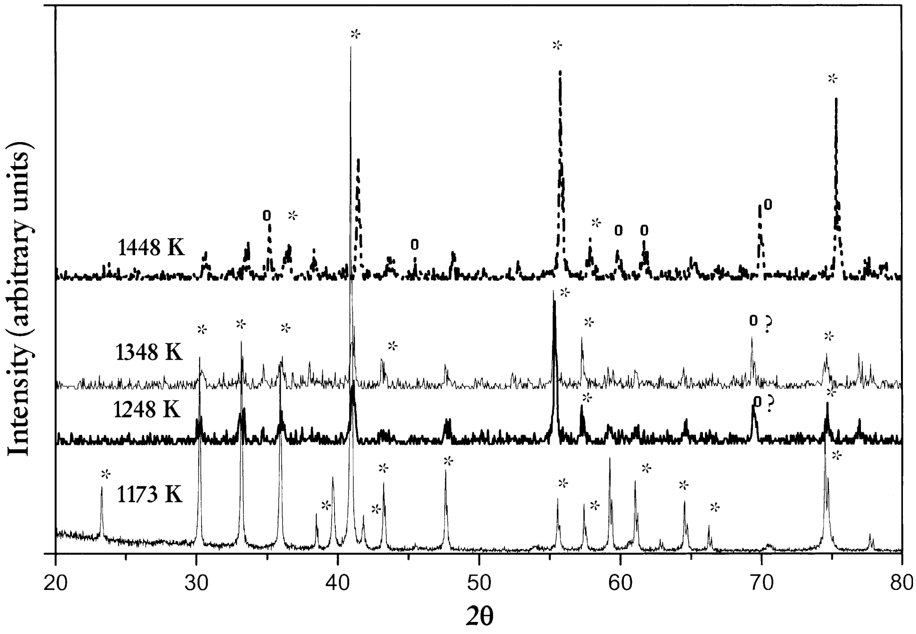

Fig. 5. High temperature XRD pattern of an alloy with the composition $Ru_{0.34}Sn_{0.66}$ annealed at 1173 K and quenched, heated to 1448 K and cooled to 298 K. Reflections pertaining to $*$ Ru_3Sn_7 and $\circ$ $RuSn_2$.

(iii) peritectic decomposition of Ru_3Sn_7 at (1538 ± 4) K

$$Ru_2Sn_3 + \text{Liquid} \xrightarrow{\text{Cooling}} Ru_3Sn_7. \quad (3)$$

(iv) an eutectic equilibrium in the tin rich end at (503 ± 1) K (composition ≃98 at.% Sn)

$$\text{Liquid} \xrightarrow{\text{Cooling}} Ru_3Sn_7 + \langle Sn \rangle. \quad (4)$$

The liquidus temperatures pertaining to the compositions 35–90 at.% Sn were measured using the conventional spot technique while the liquidus temperatures of the alloys in the range 90–100 at.% were measured using the illuminated spot technique. Complete liquefaction was not observed for the alloys in the composition range 10–35 at.% Sn up to 1823 K, which was the maximum temperature that could be attained with the apparatus employed in the present investigation. The liquidus in the composition range 35–65 at.% Sn was found to be close to the monotectic isotherm at (1570 ± 7) K.

The SEM micrographs of the alloys containing 31, 49, 69 and 90 at.% Sn are indicated in Fig. 4. The microstructures of the alloys that contained 31 and 49 at.% Sn showed the presence of almost pure ruthenium containing precipitates of Ru_2Sn_3. The alloy that contained 69 at.% Sn showed the presence of Ru_3Sn_7 and another phase whose composition was identified to be $Ru_{0.35}Sn_{0.65}$ by EDAX analysis. The microstructure of the alloy that contained 90 at.% Sn revealed the presence of Ru_3Sn_7 in a matrix that was identified to be nearly pure tin. The EDAX analysis of the alloys with the compositions $Ru_{0.6}Sn_{0.4}$ and $Ru_{0.5}Sn_{0.5}$, annealed at 1173 K for 360 h, indicated the presence of nearly pure Ru and Ru_2Sn_3. The high temperature XRD data of an alloy with a composition $Ru_{0.33}Sn_{0.67}$ is given in Fig. 5. From these data it is clear that $RuSn_2$ decomposes between 1348 and 1448 K.

4. Discussion

From Fig. 3 it is evident that the temperature corresponding to the isothermal event at (1549 ± 10) K pertains to the peritectic decomposition of Ru_2Sn_3. This value is comparable with the value of (1539 ± 4) K, reported by Perring et al. [7]. These authors suggested that the eutectic equilibrium mentioned in Eq. (5) exists in the system Ru–Sn ((1528 ± 5) K, 67 at.% Sn) and that Ru_3Sn_7 melts congruently at (1530 ± 2) K.

$$\text{Liquid} \xrightarrow{\text{Cooling}} Ru_2Sn_3 + Ru_3Sn_7. \quad (5)$$

The temperatures pertaining to complete liquefaction (open triangles) and the onset of liquefaction (open squares) obtained in this study are indicated in Fig. 3. These observations suggest the existence of a monotectic isotherm represented by Eq. (1) at (1570 ± 7) K. Kawabata et al. [5] suggested that the compound Ru_3Sn_7 may not be a congruently melting compound based on the cooling curve obtained by them for an alloy with 70.4 at.% Sn. The results obtained in the present investigation suggest that the compound Ru_3Sn_7 undergoes peritectic decomposition at (1538 ± 10) K.

The eutectic equilibrium in the tin rich end is given in Eq. (4). Perring et al. [7], suggested that this eutectic transformation occurs at (506 ± 3) K. The data obtained in this study agree well with the values reported in Ref. [7]. Even though the exact composition pertaining to this eutectic transformation could not be determined, the results obtained in the present investigation indicate that the eutectic composition is higher than 98 at.% Sn.

Susz [6] observed a liquidus boundary, which was steep in the composition range 0–35 at.% Sn and almost parallel to the composition axis in the range 35–70 at.% Sn. Kawabata et al. [5] determined the liquidus boundary in the composition range 59–63 at.% Sn using the segregation method. The data obtained by these authors [5] reveal that the compositions of the liquid alloys in equilibrium with solid ruthenium fall within a span of about 4 at.%. The data obtained in the present study indicate that the liquidus in the composition range 40–70 at.% Sn is closer to the monotectic equilibrium (1) and is not steep at least up to 40 at.% Sn as suggested by Kawabata et al. [5].

Microstructures obtained by Perring et al. [7] showed that a dense solid solution settles down in the ruthenium rich two-phase alloys comprising of a solid and a liquid phase. Such segregation could impair the results obtained in the present study. However, the stirring action brought about by the RF field employed (for heating) in the present study, prevented segregation due to gravity. In most experiments the alloy sample was flipped and the measurements were repeated, to ensure that the liquidus data obtained in this study were free from errors due to segregation of the ruthenium rich solid solution.

In the composition range 70–94 at.% Sn, Kawabata et al. [5] obtained the liquidus temperatures from thermal arrests during cooling of these alloys. These authors also measured the equilibrium tin potentials by constructing the following galvanic cell:

$$\begin{aligned}&Mo/Mo + MoO_2/ZrO_2(CaO)/\{Ru\text{–}Sn\} + CaO\\&\quad + CaSnO_4/Mo\end{aligned}$$

In the two-phase field, Ru_3Sn_7 + liquid (70–100 at.% Sn), the composition of the liquid alloy varies with the liquidus boundary. Hence, the variation of emf with temperature pertaining to alloys with different overall compositions below their liquidus temperatures would follow the same course, in the emf vs. temperature plots. A sharp change in the slope would also be discernible at the liquidus temperature. Thus Kawabata et al. [5] could verify their own liquidus data obtained by thermal arrests (in the composition range 70–94 at.% Sn) with the help of the emf data using the galvanic cell described above. Perring et al. [7] reported the liquidus data for the alloys in the composition range 70–88 at.% Sn. Susz [6] reported the liquidus data for the alloys in the composition range 75–91.5 at.% Sn. The values of all these investigations are scattered over a span of 50 K.

In all the earlier investigations [5–7], the measurements based on thermal analysis could not be successfully applied to determine the liquidus temperatures of the alloys that contained more than 95 at.% of Sn. Even in the present study, attempts to measure the liquidus temperatures using SDTA failed. The geometry of the liquidus (steep and almost parallel to the temperature axis) and the relatively low heats of fusion of alloys, that are rich in tin, make the detection of the thermal arrests pertaining to the liquidus, rather difficult in the composition range 95–100 at.% Sn.

In such instances the illuminated spot technique [17] is found to be more advantageous than DTA. Since, the former does not depend on the thermal effects for the measurement of the liquidus temperature, it is not impaired by the diminished magnitude of the thermal effect. The physical melting of the last speck of the solid could be detected owing to the higher magnification of the imaging system employed in this technique. In the composition range 95–100 at.% Sn, the data obtained in the present study are the only measurements reported so far.

From the foregoing, it is evident that these liquidus data obtained by the illuminated spot technique are more reliable because they are based on the direct visual examination of the alloys.

The results obtained in this work suggest that $RuSn_2$ decomposes by a eutectoid reaction given in Eq. (6), between 1348 and 1448 K.

$$RuSn_2 \xrightarrow{\text{Cooling}} Ru_2Sn_3 + Ru_3Sn_7. \quad (6)$$

This compound is probably formed by a peritectoid reaction given in Eq. (7), above 1500 K.

$$Ru_2Sn_3 + Ru_3Sn_7 \xrightarrow{\text{Cooling}} RuSn_2. \quad (7)$$

However, further experiments are required in order to unambiguously establish this peritectoid equilibrium.

5. Conclusions

The present study demonstrates that the steep liquidus boundary in the tin rich region 95–100 at.% Sn of the system Ru–Sn could be established using the illuminated spot technique. This testifies the utility of the new technique in determining such steep liquidus equilibria. It is also clear from the present investigation, that further investigations are required in order to establish the liquidus boundaries in the composition range 0–35 at.% Sn.

The eutectic equilibrium in the tin rich end is found to occur at (503 ± 1) K with a eutectic composition >98 at.%. The compounds Ru_2Sn_3 and Ru_3Sn_7 were found to melt peritectically at (1549 ± 10) and (1538 ± 4) K, respectively. Results obtained in the present study evidenced the presence of a monotectic isotherm at (1570 ± 7) K. High-temperature XRD results showed that the intermetallic $RuSn_2$ decomposes between 1348 and 1448 K.

Acknowledgements

The authors thank Dr V.S. Raghunathan, Associate Director, Materials Characterisation Group, IGCAR, for the keen interest he took in this work as well as for providing the facilities for carrying out the experiments. The authors express their sincere gratitude to Shri G. Panneerselvam, Fuel Chemistry Division as well as the XRD group, Materials Chemistry Division, IGCAR for their help in recording the XRD patterns at high temperatures and at room temperature.

References

[1] Hj. Matzke, Science of Advanced LMFBR Fuels, North Holland, Amsterdam, 1986.
[2] R.N. Anderson, N.A.D. Parlee, J.M. Gallagher, Nucl. Tech. 13 (1972) 29.
[3] R.J. Ackermann, E.G. Rauh, High Temp. Sci. 21 (1972) 161.
[4] O. Schwomma, H. Nowotny, A. Wittmann, Monatsh. Chem. 95 (1964) 1538.
[5] R. Kawabata, M. Myo-Chin, M. Iwase, Metall. Trans. 29B (1998) 577.
[6] C.P. Susz, thesis no. 1758, Université de Genéve, Switzerland, 1976.
[7] L. Perring, P. Feschotte, F. Bussy, J.C. Gachon, J. Alloys Compd. 245 (1996) 157.
[8] J. Charles, L. Perring, J.J. Kuntz, J.C. Gachon, J. Phase Equilib. 20 (1999) 573.
[9] S.P. Garg, R.J. Ackermann, Metall. Trans. 8A (1977) 239.
[10] S.P. Garg, R.J. Ackermann, J. Nucl. Mater. 64 (1977) 265.
[11] S.P. Garg, R.J. Ackermann, Trans. IIM 32 (1979) 62.
[12] S.P. Garg, R.J. Ackermann, Scripta Metall. 13 (1979) 611.
[13] S.P. Garg, Y.J. Bhatt, R. Venkataramani, Mater. Sci. Forum 3 (1985) 419.
[14] M.S. Chandrasekharaiah, J.L. Margrave, D. Das, in: J.F. Schooley (Ed.), Temperature – Its Measurement and

Control in Science and Industry, vol. 6, Part 1, American Institute of Physics, New York, 1992, p. 373.

[15] S.P. Garg, PhD thesis, University of Bombay, 1980.

[16] A. Awasti, Y.J. Bhatt, S.P. Garg, Mater. Sci. Tech. 7 (1996) 753.

[17] K. Ananthasivan, I. Kaliappan, P.R. Vasudeva Rao, J. Alloys Compd., submitted for publication.

[18] K. Ananthasivan, S. Anthonysamy, V. Chandramouli, I. Kaliappan, P.R. Vasudeva Rao, Trans. Powder Met. Assn. India 26 (1999) 104.

[19] A.I. Vogel, A Text Book of Quantitative Inorganic Analysis Including Elementary Instrumental Analysis, 3rd Ed., The ELBS and Longman, London, UK, 1975.

[20] S. Selvameenakshi, Project report, P.S.G. College of Arts and Science, Coimbatore, India, 2001.

[21] K. Ananthasivan, I. Kaliappan, P.R. Vasudeva Rao, Investigation on the Cu–Ni system using the 'spot technique', unpublished work.

[22] O. Knacke, O. Kubaschewski, H. Hesselmann, 2nd Ed. ASM International, Materials Park, OH, 1991.